Journal of Oceanology and Limnology
Vol. 44, No. 3, pp. 1253-1266, 2026
https://doi.org/10.1007/s00343-025-5110-4

Research Paper

Transcriptome analysis of genes and pathways associated with growth performance in eyestalks of *Exopalaemon carinicauda* under different light intensities*

Guifang JIA[1, 2, 3], Chengsong ZHANG[2, 3, **], Fuhua LI[2, 3]

[1] *Qingdao Agricultural University, School of Marine Science and Engineering, Qingdao 266109, China*
[2] *CAS and Shandong Province Key Laboratory of Experimental Marine Biology, Institute of Oceanology, Chinese Academy of Sciences, Qingdao 266071, China*
[3] *Laboratory for Marine Biology and Biotechnology, Qingdao Marine Science and Technology Center, Qingdao 266071, China*

Received Apr. 7, 2024; accepted in principle May 7, 2025; accepted for publication Jul. 15, 2025

Abstract Light is one of the important environmental factors on life activities of aquatic animals. Eyestalks are a multifunctional organ of crustaceans that conducts light signals, produces neurohormones, and regulates growth. However, the mechanism of growth regulation by light intensity remains poorly studied. We evaluated the growth performance of ridgetail white prawn (*Exopalaemon carinicauda*) under different light intensities (0, 100, 200, and 400 lx), and determined the regulatory mechanism of growth in response to light intensity through transcriptome analysis of eyestalks. Results show that light intensity at 100 lx significantly improved growth performance in growth rate, specific growth rate, and biomass increase rate, while 0-lx and 400-lx conditions inhibited the growth. A total of 931 DEGs were identified between the 100-lx and 0-lx groups, of which 411 were upregulated and 520 were downregulated. In addition, 456 DEGs were identified between groups of 100-lx and 400-lx, including 155 upregulated DEGs and 301 downregulated DEGs. The light intensity at 100 lx significantly improved the growth performance by upregulating the oxidative phosphorylation, Toll and Imd signaling pathway, and ribosome pathway, and downregulating the tyrosine metabolism, phagosome, lysosome, autophagy, and Hippo signaling pathway, whereas 0 lx and 400 lx inhibited growth in the opposite patterns. In total, eight growth-regulation-related candidate genes, i.e., *hemocyanin*, *NADH dehydrogenase*, *cytochrome c oxidase*, *ATP synthase*, *cathepsin L*, *phenoloxidase activating factor*, *CLIP domain-containing serine protease*, and *40S*/*60S ribosomal protein* were identified. The optimal light intensity for improved growth of *E. carinicauda* was about 100 lx when reared indoor. These data shall provide key information for further understanding of the regulatory mechanism of light intensity on the growth performance of this species.

Keyword: *Exopalaemon carinicauda*; eyestalk; growth performance; light intensity; transcriptome

1 INTRODUCTION

Light, including light color, intensity, and photoperiod, plays a crucial role in most life activities, such as growth, physiology, and metabolism in aquatic animals by regulating their endogenous rhythms (Shin et al., 2012). The eyestalk is a multifunctional organ of crustaceans that produces neurohormones and regulates growth, molting, and gonadal development (De Kleijn and Van Herp, 1995; Li et al., 2019). The X organ-sinus gland complex (XO-SG complex) in the eyestalk is a key neuroendocrine organ, which secretes a variety of neuropeptide hormones such as crustacean hyperglycemic hormone (CHH), molt-inhibiting hormone (MIH), maxillofacial organ-inhibiting hormone (MOIH), and gonadal development-inhibiting hormone (GIH). These hormones regulate the blood glucose level, molt,

* Supported by the China Agricultural Research System (No. CARS-48)
** Corresponding author: chszhang@qdio.ac.cn

growth, gonadal development, and many other vital physiological activities (Soyez, 1997; Gao et al., 2004).

Well-documented studies have shown that a suitable lighting environment is critical for improving growth performances, but these improving effects vary among species and developmental stages. For example, blue and green light increased the survival rate of juvenile *Melanogramus aeglefinus* (Downing, 2002), green light increased the growth rate of *Carassius carassius* (Ruchin, 2004), red light strengthened the growth performance of *Sander lucioperca* (Baekelandt et al., 2019), whereas, for *C. auratus* and *Scophthalmus maximus*, it is strengthened under blue light (Noureldin et al., 2021; Wu et al., 2021). However, white color may improve the growth performances of some crustacean species, such as *Exopalaemon carinicauda* and *Fenneropenaeus chinensis* (Wang et al., 2003; Lai et al., 2025). Light intensity also plays an important role in the physiology and behavior of aquatic animals (Shin et al., 2012). The absence of light or high light intensity exposures may trigger the stress response of aquatic animals, which in turn affects their normal physiological rhythms and metabolic activities, then increases energy consumption to cope with the stresses, and finally restricts the growth performance. It was reported that the metabolic level of *Portunus trituberculatus* was higher under a light intensity of 1 500 lx, which is beneficial for its survival and growth (Wang et al., 2014). In addition, *F. chinensis* reared at 300 lx gained the highest specific growth rate and food conversion efficiency, while the lowest one at 5 500 lx (Wang et al., 2003).

The ridgetail white prawn (*E. carinicauda*) is an important economic species in China. Due to its wide environmental adaptability, fast growth, strong reproductive capacity, and short generation cycle, it is also an important model animal for scientific research in crustacean species. Based on the foundation of CRISPR/Cas9-mediated genome editing technology in our lab, this species has been developed as a platform for the validation of important functional genes in shrimp (Gui et al., 2016; Gao et al., 2020, 2022; Miao et al., 2023). Therefore, its annual production and aquaculture in an indoor environment is vital. Inevitably, indoor lighting may be affected by weather, damage to lighting equipment, and so on.

Studies have determined the optimal environmental factors, including temperature, salinity, light color, and photoperiod (Li et al., 2013; Zhang et al., 2014; Lai et al., 2025) in this species. To date, few studies have been performed to determine the optimal light intensity for the growth and reproduction of *E. carinicauda*. Therefore, in the present study, we evaluated the growth performances under different light intensities and attempted to elucidate the regulatory mechanisms through the transcriptome analysis of the eyestalk. Results obtained from the study may improve the light factor in an indoor aquaculture system and provide helpful information for further understanding the molecular mechanisms of light regulation for the growth performances of this species.

2 MATERIAL AND METHOD

2.1 Experimental animal

Post-larvae (P1) were obtained from Xinhai Aquatic Biotech. Co., Ltd. (Huanghua, Hebei, China) and quickly transferred to our lab in the Key Laboratory of the Institute of Oceanology, Chinese Academy of Sciences. After 10 d of acclimation, P10 post-larvae (average body weight of 0.033± 0.001 g and an average body length of 0.9±0.03 cm) with no external injuries, vibrant, and complete appendages were selected and used as the experimental animals. During the acclimation period, the prawns were fed three times daily (at 09:00, 16:00, and 21:00) with newly hatched *Artemia salina* (Linnaeus, 1758) nauplii to satiation. The seawater salinity and temperature were maintained at 30–32 and 28.5±0.5 °C. A natural photoperiod (14-h light and 10-h dark) and continuous aeration were maintained.

2.2 Experimental design and sample collection

Four light intensity groups (0, 100, 200, and 400 lx) were set with three replicates for each treatment. The experimental system was covered with black shading cloths to avoid interference from indoor light. Photoperiod was set as a 12-h light and 12-h dark cycle controlled by a timer (GND-2, Bull Electrical Appliances Group Co., Ltd., Zhejiang, China), from ante meridiem 07:00 to post meridiem 19:00. For each treatment group, a 20-W TRIAC dimmable full spectrum LED light bulb (Zhongshan Mingjiou Lighting Co., Ltd., Guangzhou, China) was fixed at the center position of the upper opening of the experimental tank and used as the light source. The underwater light intensity at the bottom

in each tank was adjusted using an 86-type infinite dimming knob (TS-LSN-009, International Electrotechnical Commission) and measured by an underwater light meter (ZDS-10W, Suzhou Tianwei Instruments Co., Ltd., Jiangsu, China). We marked the water level of each experimental tank after the first measurement determined the light intensity. The light intensity at the water surface of each group was also measured, and the mean light intensity was 0, 1 200, 2 400, and 4 800 lx, respectively. 600 post-larvae were randomly selected and uniformly distributed into twelve 200-L PVC round tanks (diameter: 70 cm, height: 60 cm). During the experiment, experimental prawns were fed three times with the freshly frozen opossum shrimp in the daytime (at 9:00 and 16:00 with 3% of the body weight each time) and one more time with a commercially formulated diet at night (at 21:00 with 2% body weight). Wastes, including feces, exuviae, and dead bodies of experimental prawns, were removed every morning by siphon, and 50% of the water was changed daily. To maintain the same light intensity before and after the water change, the depth of seawater in each tank was kept at the marked level during the experimental period. The experiment lasted for 60 d. At the end of the experiment, the total wet weight and the number of surviving prawns in each tank were recorded.

Before the sample collection, we compared the growth performances among the four light intensities. It showed that light intensity at 100 lx significantly improved the growth performance of *E. carinicauda*. However, the growth of prawns reared in 200 lx showed no significant difference from the other groups. Thus, the eyestalks in 200 lx were not sampled. The compound eye and eyestalk were cut from the basement of the eye socket, then a small cut was made at the end of the compound eye, and the pigmented material was squeezed out. Eyestalks of five individuals from each light intensity were pooled as one sample, with three replications in each light level. The samples were frozen in liquid nitrogen and stored at -80 °C for further analysis.

2.3 RNA extraction, library construction, and sequencing

Total RNA was extracted from each sample according to the manufacturer's instructions using RNAiso Plus (TaKaRa, Kyoto, Japan). The concentration, purity, and integrity of the total RNA were measured using a NanoDrop 2000 (Thermo Fisher Scientific, Waltham, MA, USA) and 1% agarose gel electrophoresis. Approximately 1 μg of total RNA from each sample was preprocessed using a gDNA Eraser (TaKaRa, Kyoto, Japan), and mRNA was enriched using a conventional kit (New England Biolabs, Ipswich, MA, USA). The mRNA was fragmented and used as a template to synthesize the first-strand cDNA with random hexamers. The second-strand cDNA was synthesized by adding dNTP, RNase H, and DNA polymerase I. The purified double-stranded cDNA was end-repaired, poly(A)-tailed, and ligated to Illumina sequencing adapters. Finally, sequencing was performed on the Illumina HiSeq2500 platform by Genetron Health (Guangzhou, China).

2.4 Transcriptome assembly and unigenes functional annotation

After removing adaptor sequences, ambiguous N nucleotides (with a ratio of N>10%), low-quality sequences (with a quality score <5), and rRNA, the remaining clean reads were assembled using Trinity software (v2.8.4) as described for de novo transcriptome assembly without a reference genome, and the longest copies of redundant transcripts were regarded as unigenes. For annotation analysis, unigenes were aligned to databases using BLASTx ($E<10^{-5}$), including the National Center for Biotechnology Information non-redundant protein (Nr) database (http://www.ncbi.nlm.nih.gov) and the Orthologous Groups (COG/KOG) database (http://www.ncbi.nlm.nih.gov/COG). Gene function annotations were obtained based on the best alignment results.

2.5 Differentially expressed genes (DEGs) identification, functional enrichment and pathway analysis

RNA differential expression analysis was performed by DESeq2 software (v1.20.0) (Love et al., 2014). Genes whose false discovery rate (FDR) is below 0.05 and $|\log_2 FC|>1$ were considered DEGs. Gene Ontology (GO) functional enrichment and Kyoto Encyclopedia of Genes and Genomes (KEGG) pathway analyses of DEGs were subsequently performed using the GOSeq R package (1.12.10) with $P<0.05$.

2.6 Quantitative real-time fluorescent PCR (qRT-PCR) validation

To verify the reliability and accuracy of RNA-Seq, ten DEGs from the transcriptome data of each

tissue were selected for DEGs validation. All samples were performed in quadruplicate. The primers (Table 1) for these DEGs were designed on the Primer 3 Plus website (https://www.primer3plus.com/). Then, the relative expression levels of DEGs were detected by qRT-PCR using Eppendorf Mastercycler ep realplex (Eppendorf, Germany). The 18S rRNA gene was used as an internal reference. The qPCR program was set as follows: one cycle at 94 °C for 2 min, followed by 40 cycles: 15 s at 95 °C, 20 s at 72 °C, and finally, a 20-min melt curve step was added to test the specificity of the samples. The relative gene expression levels were calculated according to the C_t values using the formula of $2^{-\Delta\Delta Ct}$ (Livak and Schmittgen, 2001; Johnson et al., 2014). The qRT-PCR results were compared with the transcriptome data to detect the expression correlation of the selected genes.

2.7 Data calculation and statistical analysis

The growth performances were evaluated in terms of survival rate (SR), growth rate (GR), specific growth rate (SGR), and biomass increase rate (BIR). These indices were calculated as follows:

$$SR\ (\%)=100\times N_t/N_0,$$
$$GR\ (\%)=[(W_t-W_0)/W_0]\times 100,$$
$$SGR\ (\%/d)=(\ln W_t-\ln W_0)/t\times 100,$$
$$BIR\ (\%)=100\times(TW_t-TW_0)/TW_0,$$

where N_t and N_0 are the final and initial number, W_t and W_0 are the final and initial wet weight (g), t is the experimental duration (60 d), and TW_t and TW_0 are the final and initial total wet weight (g).

All data were represented as mean±S.E. (n=3). The one-way analysis of variance (ANOVA) followed by Duncan's multiple-range test to reveal the significant differences among treatments using SPSS 12.0 statistical software (SPSS Inc., Chicago, IL, USA). For all tests, $P<0.05$ was accepted as the level of statistical significance.

3 RESULT

3.1 Growth performance of *E. carinicauda* under different light intensities

The growth performances of prawns reared under different light intensities were shown in Fig.1. ANOVA confirmed that light intensity at the experimental range from 0 to 400 lx had no significant effect on SR (Fig.1a). While in terms of GR, SGR, and BIR, light intensity exhibited significant effects on these indices ($P<0.05$). Prawns reared in 100 lx showed improved growth performances than those in 0 and 400 lx ($P<0.05$), but no significant differences were observed between the 100- and 200-lx groups ($P>0.05$) (Fig.1b–d).

3.2 Transcriptome sequencing and assembly

The quality data of transcriptomic profiles were represented in Table 2. The average number of raw reads per sample was 6 797 379 600, 8 837 283 200, and 8 342 619 100 for groups of 0-, 100-, and 400-lx, respectively. After quality control of the raw reads (including the removal of adapter, containing N ratio greater than 10%, all A bases, low-quality data were removed), and the average number of clean reads per sample was 6 680 558 519, 8 651 088 051, and 8 207 697 561, which accounting for 98.28%, 97.89%, and 98.38%, respectively. The Q30 values were all greater than 94%, and the average GC content was 41.77%. In summary, the sequencing data met the requirements for subsequent data analysis.

3.3 Analysis of DEGs

The significant DEGs were shown in Fig.2. A

Table 1 The primers used for validation of DEGs by qRT-PCR

Gene	Primer sequence (5′→3′)	Annealing temperature (°C)
Phenoloxidase-activating factor 3-like	F: GGTCTGCTGTGACTCAACAA R: TCCACTCCGTTGAAGATCCT	56
Cathepsin L	F: CAGACATGACCACAGACGAG R: ACACTGTCCCTGATCCTTGA	57
Actin, clon 403	F: TACACCTTCACCACAACAGC R: TACTTGACCGTCTGGGAGTT	56
NADH dehydrogenase subunit 5	F: GTACCCACGCCTTCTTCAAA R: CGGTTTCGATGATGTGGTCT	56
Cathepsin L1	F: CAGACATGACCACAGACGAG R: ACACTGTCCCTGATCCTTGA	57
40S ribosomal protein S3a	F: CCGATGGTTACTTGCTTCGT R: TCATTTGTCTGCACCTCTCG	56

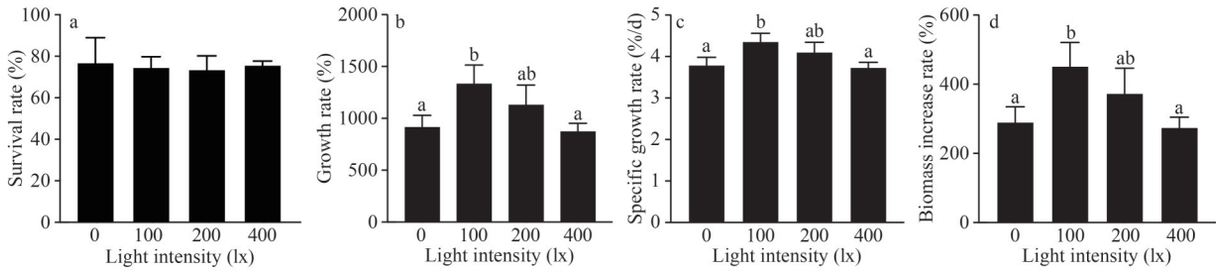

Fig.1 Effects of light intensity on growth performances of *E. carinicauda* reared for 60 d

a. survival rate; b. growth rate; c. specific growth rate; d. biomass increase rate. Values (mean±S.E., n=3) with different letters in each column indicate a significant difference (P<0.05).

Table 2 Summary of sample sequencing data quality of *E. carinicauda*

Group	Sample	Raw reads	Clean reads	Clean ratio (%)	Q30 (%)	GC (%)
0 lx	0 lx-1	6 201 366 600	6 098 799 367	98.35	94.55	41.25
	0 lx-2	7 722 040 800	7 581 424 050	98.18	94.59	41.88
	0 lx-3	6 468 731 400	6 361 452 139	98.34	94.66	41.53
100 lx	100 lx-1	8 214 211 200	8 090 096 020	98.49	94.70	41.34
	100 lx-2	7 897 459 500	7 741 839 448	98.03	94.55	42.10
	100 lx-3	10 400 178 900	10 121 328 685	97.32	94.40	42.30
400 lx	400 lx-1	7 641 963 300	7 527 266 508	98.50	96.23	41.64
	400 lx-2	7 936 970 100	7 793 701 054	98.19	94.88	42.23
	400 lx-3	9 448 923 900	9 302 125 121	98.45	95.14	42.01

total of 931 DEGs were identified between groups 100 lx and 0 lx, of which 411 were upregulated and 520 were downregulated (Fig.2a). While for the groups 100 lx and 400 lx, 456 DEGs were identified including 155 upregulated DEGs and 301 downregulated DEGs (Fig.2a). In total, 131 DEGs were intersected (Fig.2b).

3.4 Functional annotation of DEGs

Gene ontology (GO) terms could be divided into three functional categories: biological processes, molecular functions, and cellular components. For these two comparisons of 100-lx vs. 0-lx and 100-lx vs. 400-lx, 27 processes were identified in the biological processes category, comprising three biological processes (cellular process, metabolic process, and biological regulation) were the most representative and abundant subcategories. In the molecular function category, 14 subtypes were identified, comprising binding, catalytic activity, and structural molecular activity, which were most involved. In the cellular components category, only three subtypes were identified: cellular anatomical entity, protein-containing complex, and virion component. In comparison with the 0-lx group, 39 GO terms were assigned to the upregulated group

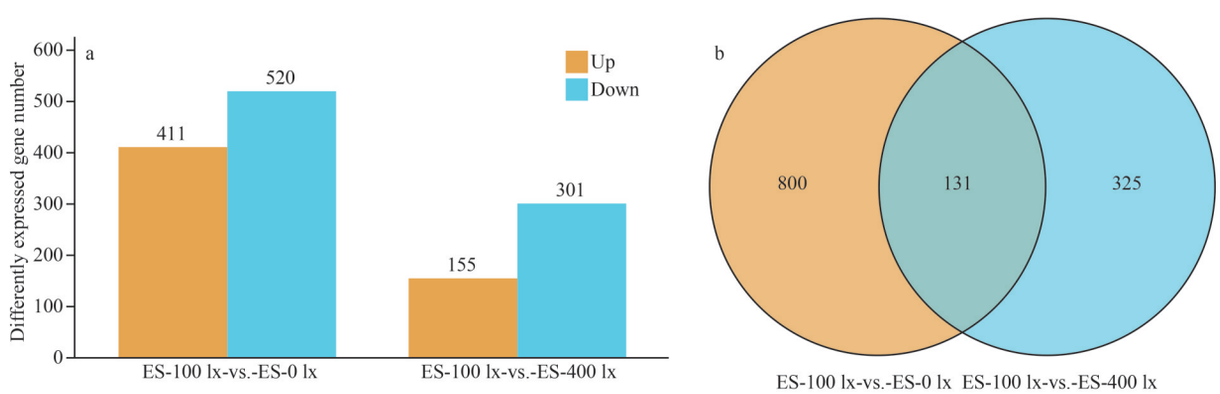

Fig.2 Distribution of DEGs with different light intensities in *E. carinicauda*

a. the number of DEGs under different light intensities; b. Venn diagram of the upregulated and downregulated genes in the 0- and 400-lx groups.

and 37 to the downregulated group in the 100-lx group (Fig.3a). While for the comparison between groups of 100-lx and 400-lx, 36 GO terms were assigned to the upregulated group and 40 to the downregulated group in the 400-lx group (Fig.3b).

3.5 KEGG enrichment analysis of DEG

KEGG enrichment analysis was performed on the DEGs, and the top 20 pathways were shown in Fig.4. In comparison with the 0-lx group, DEGs in 100-lx group were enriched into fourteen metabolism-related pathways (such as tyrosine metabolism, oxidative phosphorylation, metabolic pathway, galactose metabolism, amino sugar, and nucleotide sugar metabolism, etc.), four immunity-associated pathways (including phagosome, Toll and Imd signaling pathway, lysosome, and autophagy-animal), and two growth-related pathways: Ribosome and Hippo signaling pathway-fly (Fig.4a). Whereas for the comparison between groups of 100-lx and 400-lx, DEGs were enriched into twelve metabolism-related pathways (such as tyrosine metabolism, oxidative phosphorylation, metabolic pathway, galactose metabolism, amino sugar, and nucleotide sugar metabolism, and so on), four immunity-associated pathways (including Toll and Imd signaling pathway, phagosome, lysosome, and autophagy-animal), three signaling pathways (comprising Notch signaling pathway, TGF-beta signaling pathway, and Wnt signaling pathway), and one transporter pathway (ABC transporter) (Fig.4b).

In total, eight important pathways were selected for further analysis (Table 3). *Hemocyanin* was the most enriched DEG in the tyrosine metabolism pathway; it was significantly downregulated in the 100-lx group compared to groups of 0-lx and 400-lx. In the oxidative phosphorylation pathway, *NADH dehydrogenase*, *cytochrome c oxidase*, and *ATP synthase* were significantly upregulated in the 100-lx group than those in 0-lx and 400-lx. For the Toll and Imd signaling pathway, *phenoloxidase activation factors* and *CLIP domain-containing*

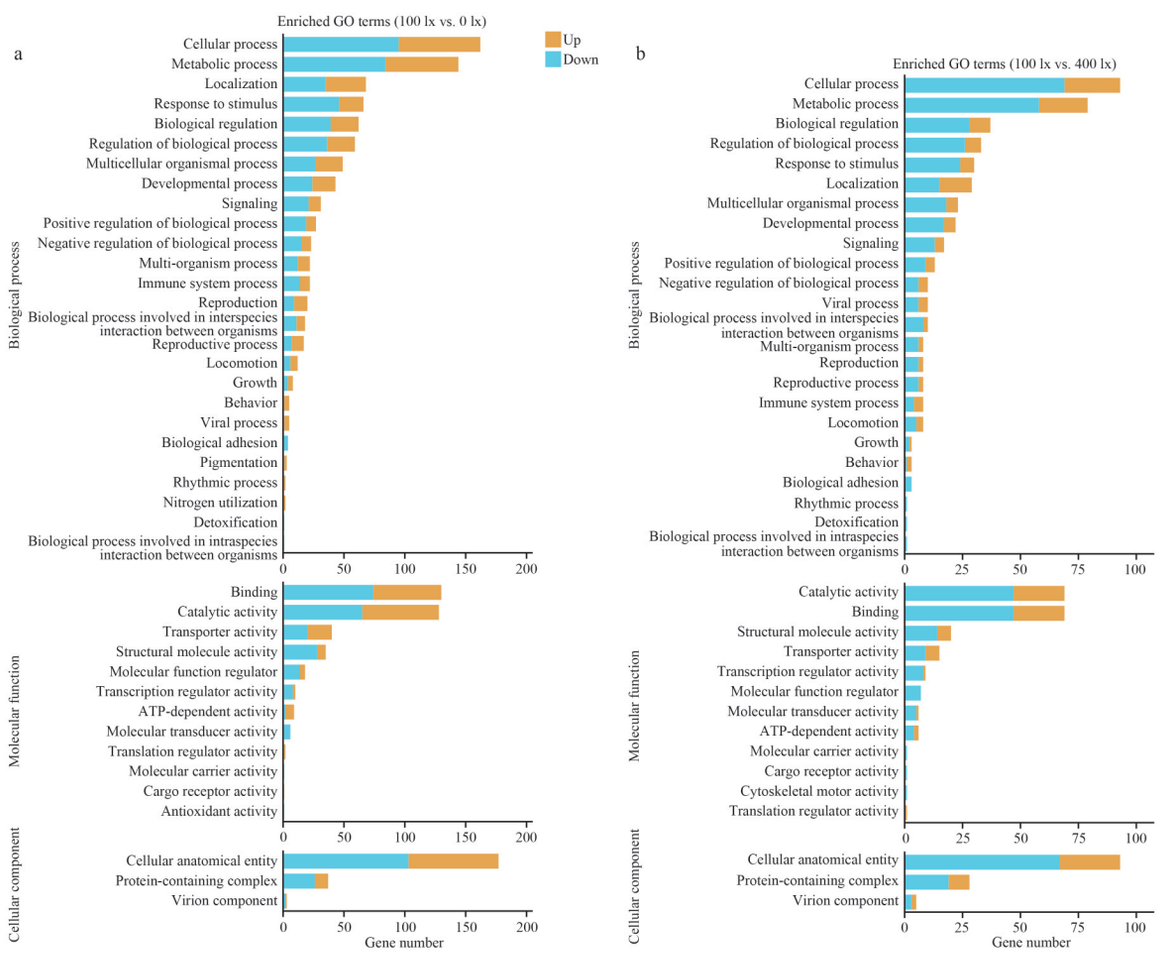

Fig.3 Gene Ontology (GO) classification showing DEGs in eyestalks of *E. caridicaude* in groups of 100-lx vs. 0-lx (a) and 100-lx vs. 400-lx (b)

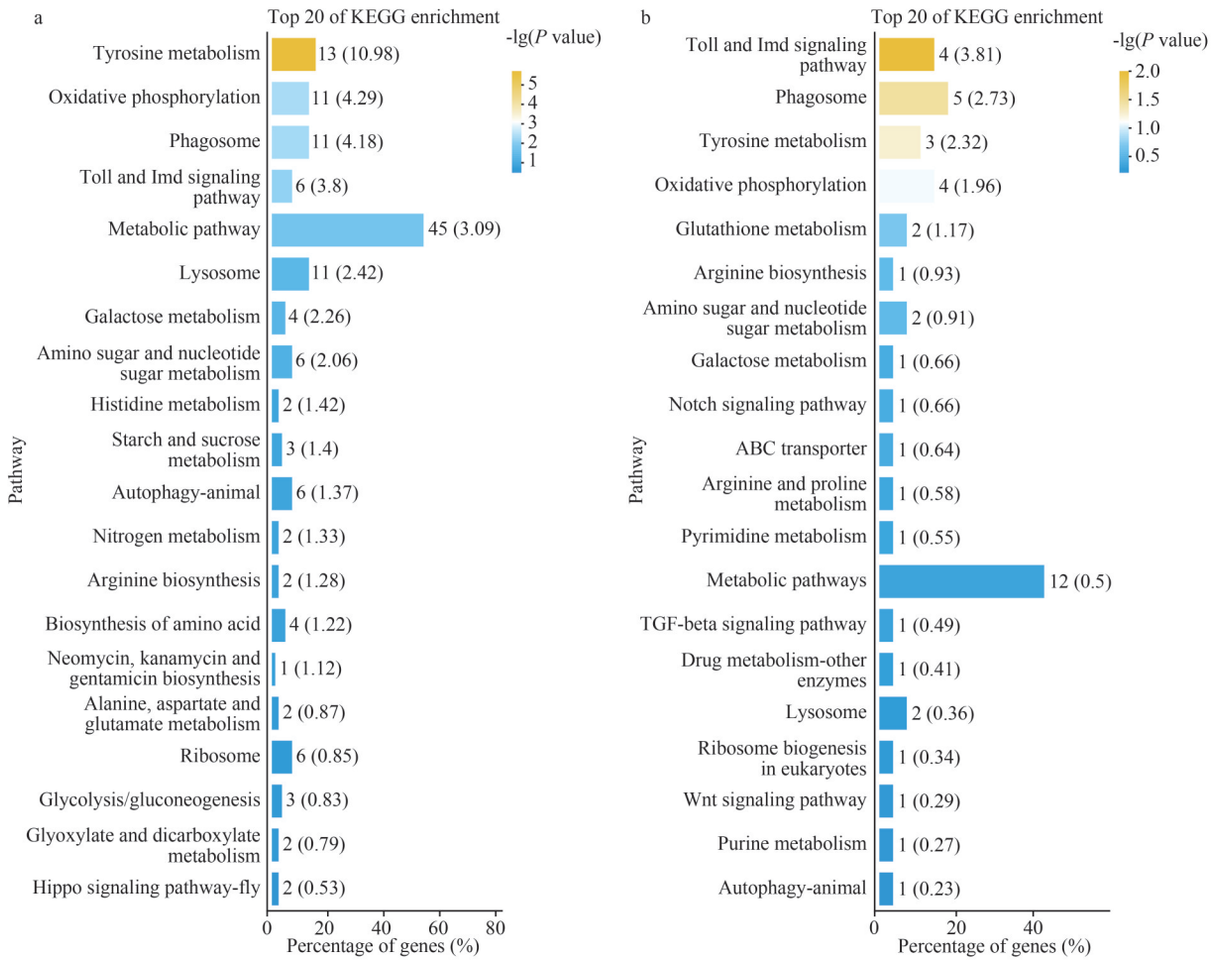

Fig.4 KEGG enrichment analysis of DEGs in eyestalks of *E. carinicauda* reared under different light intensity

a. 100 lx vs. 0 lx; b. 100 lx vs. 400 lx.

serine protease were significantly upregulated in 100-lx than those in 0-lx and 400-lx. *Cathepsin L* was most enriched in the phagosome, lysosome, and autophagy-animal. Compared with groups of 0-lx and 400-lx, this gene was significantly downregulated in 100 lx. Light intensity of 100 lx significantly activated the ribosome pathway but suppressed the Hippo signaling pathway-fly.

3.6 qRT-PCR validation

To validate the transcriptome results, qRT-PCR was used to check the transcript levels in six identified DEGs (phenoloxidase-activating factor 3-like, NADH dehydrogenase subunit 5, cathepsin L, cathepsin L1, 40S ribosomal protein S3a, and actin, clon 403). The results showed that the relative expression trends of these genes were consistent with the RNA-Seq results (Fig.5), which indicated the reliability and accuracy of sequencing quality, transcriptome assembly, and RNA-Seq expression analysis.

4 DISCUSSION

4.1 Effect of light intensity on the growth performance of *E. carinicauda*

Light is an important environmental factor that can directly or indirectly affect the growth and reproduction of aquatic animals (Guo et al., 2011; Gao et al., 2016). In the present study, light intensities at the experimental range from 0 to 400 lx showed no significant effect on survival rate of *E. carinicauda* (ranging from 71.11% at 0 lx to 76.67% at 400 lx), but the growth rate, specific growth rate, and biomass increase rate were significantly different among four light intensity groups. *E. carinicauda* grew better in 100 lx than those reared in fully dark (0 lx) and high light (400 lx) conditions. Similar results were also observed in mud crab *Scylla paramamosain* (Li et al., 2020; Chen et al., 2021) and Pacific white shrimp *Litopenaeus vannamei* (Baloi et al., 2013). It

was reported that fully dark conditions inhibit the growth in silver pomfret *Pampus Argenteus* (Hu et al., 2023), Pacific white shrimp *L. vannamei* (Fleckenstein et al., 2019), mud crab *S. paramamosain* (Chen et al., 2021), and sea cucumber *Apostichopus japonicus* (Li et al., 2019). In addition, high light intensity inhibited the growth of aquatic animals by increasing oxidative stress and inhibiting growth. For example, the growth performances of *L. vannamei* reared in high light intensity (24 W/m^2) were significantly inhibited (Fei et al., 2020). In the present study, similar results were observed, where prawns reared in 0 lx and 400 lx showed poor growth performances.

Table 3 The main pathways and DEGs identified in the eyestalks of *E. carinicauda* under different light intensities by transcriptome

ID	Description	100 lx vs. 0 lx		100 lx vs. 400 lx	
		Fold change	*P* value	Fold change	*P* value
	Metabolism-related pathway				
Tyrosine metabolism					
Unigene0026267	Hemocyanin	16.806	0.038 9	\	\
Unigene0131190	Hemocyanin	1050	0.011 8	\	\
Unigene0075883	Hemocyanin beta subunit 1	215.67	0.008 1	\	\
Unigene0008222	Hemocyanin	14.59	3.31E-06	\	\
Unigene0087406	Hemocyanin	22.283	2.16E-22	4.774	0.001
Unigene0008220	Hemocyanin	18.779	4.49E-06	6.134 2	0.027 5
Unigene0112173	Hemocyanin	9.905 8	0.007 8	\	\
Unigene0008219	Hemocyanin	776.67	0.021 1	\	\
Unigene0105663	Hemocyanin	1 416	0.009 8	\	\
Unigene0032338	HcL3	19.994	9.80E-06	\	\
Unigene0008221	HcL3	33.143	6.25E-05	\	\
Unigene0051860	HcL3	34.063	0.000 5	\	\
Unigene0112338	Homogentisate 1,2-dioxygenase-like	0.479 3	0.002 5	\	\
Unigene0138824	Aromatic-L-amino-acid decarboxylase-like	\	\	0.438 8	0.000 3
Oxidative phosphorylation					
Unigene0117526	ATP synthase FO subunit 6, partial	0.003 6	0.000 3	0.061 3	0.039 5
Unigene0030629	Cytochrome c oxidase subunit I	0.003 1	0.001 2	\	\
Unigene0059831	Cytochrome c oxidase subunit II	0.003 8	0.008 5	\	\
Unigene0117527	Cytochrome c oxidase subunit III	0.007 6	0.014 4	\	\
Unigene0111054	Cytochrome b, partial	0.000 2	0.033 9	\	\
Unigene0028206	NADH dehydrogenase subunit 2	0.000 2	0.041 4	\	\
Unigene0104025	NADH dehydrogenase subunit 3	0.000 7	0.023 0	0.000 7	0.020 1
Unigene0031882	NADH dehydrogenase subunit 4	0.002 2	0.005 7	\	\
Unigene0003055	NADH dehydrogenase subunit 5	0.000 5	0.036 6	0.039 5	0.047 6
	Immunity-associated pathway				
Phagosome					
Unigene0106075	Actin, clone 403	6.942 4	1.49E-05	\	\
Unigene0040719	Macronuclear actin	631.33	0.000 3	\	\
Unigene0047444	Cathepsin L2	13.08 2	0.017 9	\	\
Unigene0022801	Cathepsin L	6.967 1	0.000 2	3.618 9	0.027 1
Unigene0116269	Cathepsin L1	22.974	0.000 4	\	\
Unigene0098731	Putative cathepsin L	192.67	0.037 1	\	\
Unigene0036952	Lysosome-associated membrane glycoprotein 1-like	199.67	0.024 2	\	\
Unigene0105665	Nitric oxide synthase	\	\	0.367 9	0.012 6
Unigene0019672	Tubulin alpha-1 chain-like	0.498 1	3.74E-09	\	\

To be continued

Table 3 Continued

ID	Description	100 lx vs. 0 lx		100 lx vs. 400 lx	
		Fold change	*P* value	Fold change	*P* value
Unigene0030687	Vacuolar ATP synthase subunit, putative	21.525	0.028 4	\	\
Unigene0131216	Low affinity immunoglobulin epsilon Fc receptor	0.196 9	0.036 8	0.109 6	0.013 3
Lysosome					
Unigene0022801	Cathepsin l	6.967 1	0.000 2	3.618 9	0.027 1
Unigene0116269	Cathepsin L1	22.974	0.000 4	\	\
Unigene0047444	Cathepsin L2	13.082	0.017 9	\	\
Unigene0141436	Cathepsin b	22.125	0.006 6	\	\
Unigene0045829	Legumain-like protein	25.733	0.000 3	8.851 5	0.019 5
Unigene0080976	Legumain-like protein	32.068	0.005 6	\	\
Unigene0064235	Sialin-like	3.057 7	0.015 8	\	\
Unigene0036952	Lysosome-associated membrane glycoprotein 1-like	199.67	0.024 2	\	\
Unigene0094226	Alpha-L-fucosidase-like	82.000	0.030 2	\	\
Unigene0064236	Sialin-like	3.132 6	0.032 7	\	\
Unigene0098731	Putative cathepsin L	192.67	0.037 1	\	\
Autophagy-animal					
Unigene0022801	Cathepsin L	6.967 1	0.000 2	3.617 8	0.027 1
Unigene0116269	Cathepsin L1	22.974	0.000 4	\	\
Unigene0141436	Cathepsin B	22.125	0.006 6	\	\
Unigene0047444	Cathepsin L2	13.082	0.017 9	\	\
Unigene0036952	Lysosome-associated membrane glycoprotein 1-like	199.67	0.024 2	\	\
Unigene0098731	Putative cathepsin L	192.67	0.037 1	\	\
Toll and Imd signaling pathway					
Unigene0111538	CLIP domain-containing serine protease 2-like	0.415 3	8.40E-05	0.470 9	0.002 0
Unigene0071192	CLIP domain-containing serine protease 2-like	0.416 3	0.035 9	\	\
Unigene0016953	Phenoloxidase-activating factor 3-like	\	\	0.420 2	0.017 0
Unigene0061260	Phenoloxidase-activating factor 1-like isoform X2	0.368 9	4.54E-09	0.452 6	1.16E-05
Unigene0099085	Phenoloxidase-activating factor 1-like isoform X1	0.479 5	1.26E-05	\	\
Unigene0081827	Phenoloxidase-activating factor 3-like 1	0.344 6	0.038	\	\
Unigene0081826	Phenoloxidase-activating factor 3-like	0.434 1	0.004 3	0.420 6	0.032 9
	Growth-related pathway				
Ribosome					
Unigene0053907	40S ribosomal protein S17	0.001 3	0.029 2	\	\
Unigene0110316	40S ribosomal protein S2	0.015 5	0.037 2	\	\
Unigene0080811	40S ribosomal protein S3a	0.016 9	0.038 3	\	\
Unigene0015470	60S ribosomal protein L7-like	0.023 2	0.046 5	\	\
Unigene0102153	60S ribosomal protein L11 isoform X2	0.001 6	0.043 3	\	\
Unigene0125724	60S acidic ribosomal protein P0-like	0.000 5	0.005 0	\	\
Unigene0062205	60S ribosomal protein L12-like 1	\	\	0.304 1	0.000 3
Hippo signaling pathway-fly					
Unigene0040719	Macronuclear actin	631.33	0.000 3	\	\
Unigene0106075	Actin, clone 403	6.942 4	1.49E-05	\	\

\ means non-DEGs.

4.2 Effect of light intensity on metabolism-related pathways of *E. carinicauda*

Among the metabolism-related pathways enriched in the 100-lx group, tyrosine metabolism was the most affected one and *hemocyanin* was enriched into this pathway. It was reported that involved in the biosynthesis of melanin, exerting antioxidant capacity and radiation protection (del Marmol and Beermann, 1996). Hemocyanin is a

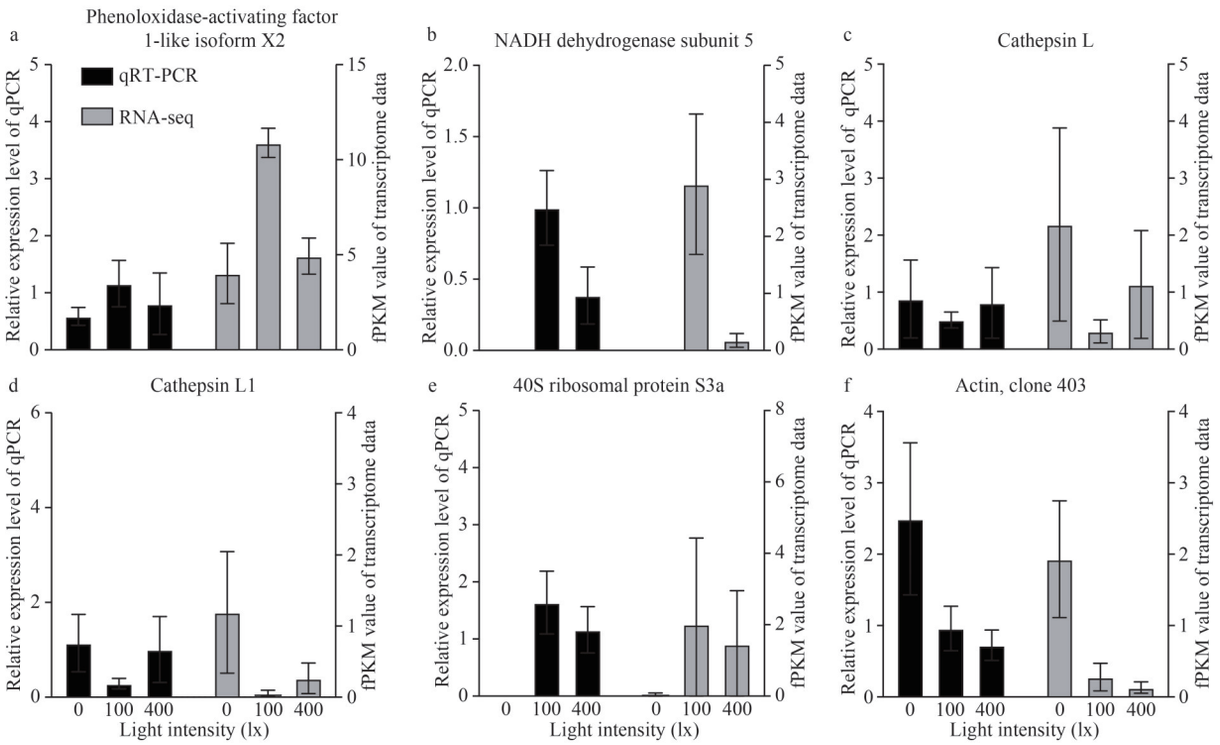

Fig.5 Comparison of RNA-seq and qRT-PCR expression profiles of six selected DEGs in *E. carinicauda*

multifunctional molecule and plays pivotal roles in biological and catalytic processes, including oxygen transport, catalysis, and oxidative chemistry (Coates and Costa-Paiva, 2020). Studies have shown that *hemocyanin* showed significantly up-regulated expression patterns under stress conditions such as hypoxia (Zhou et al., 2014) and low salt (Weiland and Mangum, 1975). In this study, the mean expression level of *hemocyanin* in 0-lx and 400-lx was significantly increased by 392.42- and 4.45-fold than that in the 100-lx group. These results indicated that fully dark and high light conditions may trigger a stress response, hence, more energy was consumed to cope with the stress factors, which in turn suppressed their growth.

Oxidative phosphorylation is a coupling reaction between the energy released by the body, ATP, and inorganic phosphate synthesis through the respiratory chain (Gonzalvez et al., 2005). The destruction and mutation of any component in the oxidative phosphorylation pathway can lead to impaired ATP production and intensified oxidative stress (Barreto and Burton, 2013), and oxidative stress is closely related to apoptosis (Cheng et al., 2019). In this pathway, three types of genes (*NADH dehydrogenase*, *cytochrome c oxidase*, and *ATP synthase*) were significantly upregulated in 100 lx than in 0-lx and 400-lx groups, but the fold change in the 0-lx group was significantly higher than that of the 400-lx group. NADH dehydrogenase is one of the core subunits of mitochondrial respiratory chain complex I, involved in electron transport and proton pumping from NADH to ubiquinone. NADH-ubiquinone oxidoreductase and cytochrome c oxidase participate in the transfer of electrons to oxygen and, thus, are considered the key components of the respiratory chain (Hatefi, 1985). ATP synthase is involved in the proton flow, which releases energy to the enzyme rotor to catalyze ATP synthesis (Ganetzky et al., 2019). Studies have shown that the reduced ATP synthase FO subunit leads to defects in complex V assembly and function (Jonckheere et al., 2008). In this study, the significant up-regulation of *NADH dehydrogenase*, *cytochrome c oxidase*, and *ATP synthase* indicated that the process of the respiratory chain and energy synthesis was accelerated in the medium light conditions. In this case, more energy can be allocated to growth, then exhibit better growth performance. On the contrary, the fully dark (0 lx) and higher light (400 lx) conditions inhibited this energy generation process and finally suppressed the growth performance.

4.3 Effect of light intensity on immunity-associated pathways of *E. carinicauda*

The innate defense system of crustaceans consists of humoral and cellular immunity (Li and Xiang, 2013). When organisms are exposed to environmental stress, immunity defense mechanisms are usually activated, and cell death/apoptosis is triggered to defend against stress (Lu et al., 2016). Cathepsin L, a cysteine protease, is involved in many biological processes, such as antigen presentation, cell death/apoptosis, and pathogen infection (Burton et al., 2015; Braden et al., 2017; Voronina et al., 2024). In the present study, *cathepsin L* was significantly upregulated and enriched in three significantly upregulated pathways, including phagosome, lysosome, and autophagy-animal, both in the 0-lx and 400-lx groups, suggesting that these were the key pathways for the response of the immune system to light stress. The excessive production of cathepsin L may trigger an oxidative response and autophagy, finally induce cell death and inhibiting cell growth. In a study of nitrogen and phosphorus stress performed in *L. vannamei*, the phagosome and lysosomal pathways were also enriched and significantly upregulated, which finally affected its growth through the synergistic effect (Zhao et al., 2025).

In terms of Toll and Imd signaling pathway, when ligands bind to Toll receptors, the Toll pathway is responsible for defending against Gram-positive bacteria or fungi, eventually leading to the activation of dorsal-associated immune factors. It is also involved in the developmental process (Belvin and Anderson, 1996; Qiu et al., 1998) and immunity (Lemaitre et al., 1996; Valanne et al., 2011). The Imd pathway controls the drug resistance of Gram-negative bacterial infections (Reumer et al., 2010; Valanne et al., 2011). In this pathway, two genes (*phenoloxidase-activating factor* and *serine protease*) were significantly upregulated in 100-lx groups. In general, phenoloxidase (PO) is present in an inactive form called prophenoloxidase (pro-PO) in the hemolymph of invertebrates (Cerenius and Söderhäll, 2004). Through a specific serine protease cascade reaction, the enzyme activates phenoloxidase activating factor into phenologen activating enzyme (Ashida, 1971; Ashida and Brey, 1995). Phenoloxidase-activating factor directly affects PO activity and the immune defense mechanism and plays an important role in the non-specific immune defense of marine invertebrates (Cerenius and Söderhäll, 2004). In addition, PO is also involved in the hardening of insect cuticle (Andersen et al., 1996). Studies have shown that PO is a key enzyme in the molting growth of silkworm (Wang et al., 2013). Similar results were obtained in the short-tail crab (*Cancer magister*), where PO played an important role in the hardening of the new molting exoskeleton and the immune response (Terwilliger and Ryan, 2006). In the present study, the expression of *phenoloxidase-activating factor* and *serine protease* was significantly upregulated in 100-lx group, which was consistent with their better growth performances and may result in a high frequency of molting and the growth rate of the shell of the *E. carinicauda*, thus improving their growth.

4.4 Effect of light intensity on growth-related pathways of *E. carinicauda*

In this study, two growth-related pathways, including the ribosome pathway and the Hippo signaling pathway-fly, were screened by KEGG analysis in the 100-lx group. Ribosomes are large, complex particles composed of RNA and proteins that are the sites of protein biosynthesis and processing in cells (Li et al., 2021). In addition, it serves as a starting step for several translation-related functions, such as protein folding and defects or uninterrupted mRNA degradation (Barranger et al., 2019). Studies have determined that ribosome function is closely related to the improvement of growth performance and immunity in aquatic animals (Li et al., 2020; Hou et al., 2021). In this study, six DEGs encoding ribosomal proteins were significantly upregulated and enriched in the ribosome pathway in the 100-lx group, which suggests a positive effect on protein biosynthesis for *E. carinicauda* in medium-light conditions. In the 400-lx group, one DEG, namely *60S ribosomal protein L12-like 1*, was significantly downregulated than that in the 100-lx group, so the growth was suppressed in this light level.

Hippo signaling is an evolutionarily conserved signaling pathway that controls organ size. It is critical for monitoring tissue growth during animal development (Ye et al., 2012). In the 100-lx group, two downregulated DEGs were enriched in this pathway. These results indicate that cellular growth and cell division were somewhat suppressed and cell apoptosis was activated in fully dark conditions, but the mechanisms of these actions require further study.

5 CONCLUSION

In the present study, the effects of light intensities (0, 100, 200, and 400 lx) on the growth performances of ridgetail white prawn (*Exopalaemon carinicauda*) were evaluated, and the pathways and genes associated with growth regulation were identified by comparative transcriptome analysis of eyestalk in response to different light intensity. To our knowledge, this is the first transcriptome analysis of eyestalks to reveal the regulatory mechanism of growth in *E. carinicauda* under different light intensities. Results showed that 100 lx significantly improved the growth in this species by upregulating oxidative phosphorylation, Toll and Imd signaling pathway, and ribosome, and downregulating tyrosine metabolism, phagosome, lysosome, autophagy, and Hippo signaling pathway. However, the light intensity at 0 and 400 lx inhibited its growth by the contrary regulatory trends. In total, eight growth-regulation-related candidate genes, including *hemocyanin*, *NADH dehydrogenase*, *cytochrome c oxidase*, *ATP synthase*, *cathepsin L*, *phenoloxidase activating factor*, *CLIP domain-containing serine protease*, and *40S*/*60S ribosomal protein*, were identified. These data may provide important information for further understanding the molecular mechanisms of light regulation for the growth in this species. We suggested that a medium light intensity of approximately 100 lx should be supplied to improve the growth performance of *E. carinicauda* reared in an indoor condition.

6 DATA AVAILABILITY STATEMENT

The data generated and/or analyzed during the current study are available from the corresponding author on request.

7 ACKNOWLEDGMENT

We would like to thank all the reviewers for their diligent assessment and advice, which greatly improved the manuscript.

References

Andersen S O, Peter M G, Roepstorff P. 1996. Cuticular sclerotization in insects. *Comparative Biochemistry and Physiology Part B*: *Biochemistry and Molecular Biology*, **113**(4): 689-705, https://doi.org/10.1016/0305-0491(95)02089-6.

Ashida M. 1971. Purification and characterization of pre-phenoloxidase from hemolymph of the silkworm *Bombyx mori*. *Archives of Biochemistry and Biophysics*, **144**(2): 749-762, https://doi.org/10.1016/0003-9861(71)90383-3.

Ashida M, Brey P T. 1995. Role of the integument in insect defense: pro-phenol oxidase cascade in the cuticular matrix. *Proceedings of the National Academy of Sciences of the United States of America*, **92**(23): 10698-10702, https://doi.org/10.1073/pnas.92.23.10698.

Baekelandt S, Mandiki S N M, Schmitz M et al. 2019. Influence of the light spectrum on the daily rhythms of stress and humoral innate immune markers in pikeperch *Sander lucioperca*. *Aquaculture*, **499**: 358-363, https://doi.org/10.1016/j.aquaculture.2018.09.046.

Baloi M, Arantes R, Schveitzer R et al. 2013. Performance of Pacific white shrimp *Litopenaeus vannamei* raised in biofloc systems with varying levels of light exposure. *Aquacultural Engineering*, **52**: 39-44, https://doi.org/10.1016/j.aquaeng.2012.07.003.

Barranger A, Langan L M, Sharma V et al. 2019. Antagonistic interactions between Benzo[a]pyrene and fullerene (C_{60}) in toxicological response of marine mussels. *Nanomaterials*, **9**(7): 987, https://doi.org/10.3390/nano9070987.

Barreto F S, Burton R S. 2013. Elevated oxidative damage is correlated with reduced fitness in interpopulation hybrids of a marine copepod. *Proceedings of the Royal Society B*: *Biological Sciences*, **280**(1767): 20131521, https://doi.org/10.1098/rspb.2013.1521.

Belvin M P, Anderson K V. 1996. A CONSERVED SIGNALING PATHWAY: the *Drosophila* toll-dorsal pathway. *Annual Review of Cell and Developmental Biology*, **12**: 393-416, https://doi.org/10.1146/annurev.cellbio.12.1.393.

Braden L M, Sutherland B J G, Koop B F et al. 2017. Enhanced transcriptomic responses in the Pacific salmon louse *Lepeophtheirus salmonis oncorhynchi* to the non-native Atlantic Salmon *Salmo salar* suggests increased parasite fitness. *BMC Genomics*, **18**(1): 110, https://doi.org/10.1186/s12864-017-3520-1.

Burton L J, Smith B A, Smith B N et al. 2015. Muscadine grape skin extract can antagonize Snail-cathepsin L-mediated invasion, migration and osteoclastogenesis in prostate and breast cancer cells. *Carcinogenesis*, **36**(9): 1019-1027, https://doi.org/10.1093/carcin/bgv084.

Cerenius L, Söderhäll K. 2004. The prophenoloxidase-activating system in invertebrates. *Immunological Reviews*, **198**(1): 116-126, https://doi.org/10.1111/j.0105-2896.2004.00116.x.

Chen S J, Migaud H, Shi C et al. 2021. Light intensity impacts on growth, molting and oxidative stress of juvenile mud crab *Scylla paramamosain*. *Aquaculture*, **545**: 737159, https://doi.org/10.1016/j.aquaculture.2021.737159.

Cheng C H, Ma H L, Su Y L et al. 2019. Ammonia toxicity in the mud crab (*Scylla paramamosain*): the mechanistic insight from physiology to transcriptome analysis. *Ecotoxicology and Environmental Safety*, **179**: 9-16, https://doi.org/10.1016/j.ecoenv.2019.04.033.

Coates C J, Costa-Paiva E M. 2020. Multifunctional roles of hemocyanins. *In*: Hoeger U, Harris J R eds. Vertebrate

and Invertebrate Respiratory Proteins, Lipoproteins and other Body Fluid Proteins. Springer, Cham. p.233-250, https://doi.org/10.1007/978-3-030-41769-7_9.

De Kleijn D P V, Van Herp F. 1995. Molecular biology of neurohormone precursors in the eyestalk of Crustacea. *Comparative Biochemistry and Physiology Part B*: *Biochemistry and Molecular Biology*, **112**(4): 573-579, https://doi.org/10.1016/0305-0491(95)00126-3.

del Marmol V, Beermann F. 1996. Tyrosinase and related proteins in mammalian pigmentation. *FEBS Letters*, **381**(3): 165-168, https://doi.org/10.1016/0014-5793(96)00109-3.

Downing G. 2002. Impact of spectral composition on larval haddock, *Melanogrammus aeglefinus* L., growth and survival. *Aquaculture Research*, **33**(4): 251-259, https://doi.org/10.1046/j.1355-557x.2002.00668.x.

Fei F, Gao X Q, Wang X Y et al. 2020. Effect of spectral composition on growth, oxidative stress responses, and apoptosis-related gene expression of the shrimp, *Penaeus vannamei*. *Aquaculture Reports*, **16**: 100267, https://doi.org/10.1016/j.aqrep.2019.100267.

Fleckenstein L J, Tierney T W, Fisk J C et al. 2019. Effects of supplemental LED lighting on water quality and Pacific white shrimp (*Litopenaeus vannamei*) performance in intensive recirculating systems. *Aquaculture*, **504**: 219-226, https://doi.org/10.1016/j.aquaculture.2019.01.066.

Ganetzky R D, Stendel C, McCormick E M et al. 2019. *MT-ATP6* mitochondrial disease variants: phenotypic and biochemical features analysis in 218 published cases and cohort of 14 new cases. *Human Mutation*, **40**(5): 499-515, https://doi.org/10.1002/humu.23723.

Gao C L, Sun J S, Xiang J H et al. 2004. Electrophysiological study of neurosecretory neurons in eyestalk of shrimp *Fenneropenaeus chinensis*. *Oceanologia et Limnologia Sinica*, **35**(6): 555-561, https://doi.org/10.3321/j.issn:0029-814X.2004.06.012. (in Chinese with English abstract)

Gao X L, Zhang M, Li X et al. 2016. Effects of LED light quality on the growth, metabolism, and energy budgets of *Haliotis discus discus*. *Aquaculture*, **453**: 31-39, https://doi.org/10.1016/j.aquaculture.2015.11.033.

Gao Y, Zhang X J, Yuan J B et al. 2022. CRISPR/Cas9-mediated mutation on an insulin-like peptide encoding gene affects the growth of the ridgetail white prawn *Exopalaemon carinicauda*. *Frontiers in Endocrinology*, **13**: 986491, https://doi.org/10.3389/fendo.2022.986491.

Gao Y, Zhang X X, Zhang X J et al. 2020. CRISPR/Cas9-mediated mutation reveals *Pax6* is essential for development of the compound eye in Decapoda *Exopalaemon carinicauda*. *Developmental Biology*, **465**(2): 157-167, https://doi.org/10.1016/j.ydbio.2020.07.001.

Gonzalvez F, Pariselli F, Dupaigne P et al. 2005. tBid interaction with cardiolipin primarily orchestrates mitochondrial dysfunctions and subsequently activates Bax and Bak. *Cell Death & Differentiation*, **12**(6): 614-626, https://doi.org/10.1038/sj.cdd.4401571.

Gui T S, Zhang J Q, Song F G et al. 2016. CRISPR/Cas9-mediated genome editing and mutagenesis of *EcChi4* in *Exopalaemon carinicauda*. *G3 Genes|Genomes|Genetics*, **6**(11): 2757-2764, https://doi.org/10.1534/g3.116.034082.

Guo B, Wang F, Dong S L et al. 2011. The effect of rhythmic light color fluctuation on the molting and growth of *Litopenaeus vannamei*. *Aquaculture*, **314**(1-4): 210-214, https://doi.org/10.1016/j.aquaculture.2011.02.023.

Hatefi Y. 1985. The mitochondrial electron transport and oxidative phosphorylation system. *Annual Review of Biochemistry*, **54**: 1015-1069, https://doi.org/10.1146/annurev.bi.54.070185.005055.

Hou C H, Song S G, Zhu L L et al. 2021. Growth, immunity, and transcriptome response to dietary Wnt/β-catenin pathway activator TWS119 in *Penaeus vannamei*. *Frontiers in Marine Science*, **8**: 685429, https://doi.org/10.3389/fmars.2021.685429.

Hu J B, Sun J C, Zhang M et al. 2023. Effects of different light intensity on growth, feeding, retinal structure and expression of vision-related genes of silver pomfret. *Aquaculture Reports*, **30**: 101631, https://doi.org/10.1016/j.aqrep.2023.101631.

Johnson G, Nour A A, Nolan T et al. 2014. Minimum information necessary for quantitative real-time PCR experiments. *In*: Biassoni R, Raso A eds. Quantitative Real-Time PCR. Humana Press, New York. p.5-17, https://doi.org/10.1007/978-1-4939-0733-5_2.

Jonckheere A I, Hogeveen M, Nijtmans L G J et al. 2008. A novel mitochondrial *ATP8* gene mutation in a patient with apical hypertrophic cardiomyopathy and neuropathy. *Journal of Medical Genetics*, **45**(3): 129-133, https://doi.org/10.1136/jmg.2007.052084.

Lai X F, Guo X F, Wu C et al. 2025. Different light colors have different effects on the growth, digestion, non-specific immunity, and ovarian maturation of female *Exopalaemon carinicauda*. *Aquaculture International*, **33**(2): 129, https://doi.org/10.1007/s10499-024-01819-3.

Lemaitre B, Nicolas E, Michaut L et al. 1996. The dorsoventral regulatory gene cassette *spätzle*/*toll*/*cactus* controls the potent antifungal response in Drosophila adults. *Cell*, **86**(6): 973-983, https://doi.org/10.1016/S0092-8674(00)80172-5.

Li C L, Zhao W, Qin C X et al. 2021. Comparative transcriptome analysis reveals changes in gene expression in sea cucumber (*Holothuria leucospilota*) in response to acute temperature stress. *Comparative Biochemistry and Physiology Part D*: *Genomics and Proteomics*, **40**: 100883, https://doi.org/10.1016/j.cbd.2021.100883.

Li F H, Xiang J H. 2013. Recent advances in researches on the innate immunity of shrimp in China. *Developmental & Comparative Immunology*, **39**(1-2): 11-26, https://doi.org/10.1016/j.dci.2012.03.016.

Li L, Zhang Y S, Dong S L et al. 2019. Effects of light intensity on larval development and juvenile growth of sea cucumber *Apostichopus japonicus*. *Aquaculture Research*, **50**(9): 2333-2340, https://doi.org/10.1111/are.14113.

Li N, Zhou J M, Wang H et al. 2020. Transcriptome analysis of genes and pathways associated with metabolism in *Scylla paramamosain* under different light intensities

during indoor overwintering. *BMC Genomics*, **21**(1): 775, https://doi.org/10.1186/s12864-020-07190-w.

Li Z G, Zhang C S, Zhang Y et al. 2013. Effects of temperature on embryonic and larval development of the *Exopalaemon carinicauda* (Holthuis). *Marine Sciences*, **37**(10): 9-16. (in Chinese with English abstract)

Livak K J, Schmittgen T D. 2001. Analysis of relative gene expression data using real-time quantitative PCR and the $2^{-\Delta\Delta C_T}$ method. *Methods*, **25**(4): 402-408, https://doi.org/10.1006/meth.2001.1262.

Love M I, Huber W, Anders S. 2014. Moderated estimation of fold change and dispersion for RNA-seq data with DESeq2. *Genome Biology*, **15**(12): 550, https://doi.org/10.1186/s13059-014-0550-8.

Lu X, Kong J, Luan S et al. 2016. Transcriptome analysis of the hepatopancreas in the Pacific white shrimp (*Litopenaeus vannamei*) under acute ammonia stress. *PLoS One*, **11**(10): e0164396, https://doi.org/10.1371/journal.pone.0164396.

Miao M, Li S H, Yuan J B et al. 2023. CRISPR/Cas9-mediated gene mutation of *EcIAG* leads to sex reversal in the male ridgetail white prawn *Exopalaemon carinicauda*. *Frontiers in Endocrinology*, **14**: 1266641, https://doi.org/10.3389/fendo.2023.1266641.

Noureldin S M, Diab A M, Salah A S et al. 2021. Effect of different monochromatic LED light colors on growth performance, behavior, immune-physiological responses of gold fish, *Carassius auratus*. *Aquaculture*, **538**: 736532, https://doi.org/10.1016/j.aquaculture.2021.736532.

Qiu P, Pan P C, Govind S. 1998. A role for the *Drosophila* Toll/Cactus pathway in larval hematopoiesis. *Development*, **125**(10): 1909-1920, https://doi.org/10.1242/dev.125.10.1909.

Reumer A, Von Loy T, Schoofs L. 2010. The complexity of *Drosophila* innate immunity. *Invertebrate Survival Journal*, **7**(1): 32-44.

Ruchin A B. 2004. Influence of colored light on growth rate of juveniles of fish. *Fish Physiology and Biochemistry*, **30**(2): 175-178, https://doi.org/10.1007/s10695-005-1263-4.

Shin H S, Lee J, Choi C Y. 2012. Effects of LED light spectra on the growth of the yellowtail clownfish *Amphiprion clarkii*. *Fisheries Science*, **78**(3): 549-556, https://doi.org/10.1007/s12562-012-0482-8.

Soyez D. 1997. Occurrence and diversity of neuropeptides from the crustacean hyperglycemic hormone family in arthropods: a short review. *Annals of the New York Academy of Sciences*, **814**(1): 319-323, https://doi.org/10.1111/j.1749-6632.1997.tb46174.x.

Terwilliger N B, Ryan M C. 2006. Functional and phylogenetic analyses of phenoloxidases from brachyuran (*Cancer magister*) and branchiopod (*Artemia franciscana*, *Triops longicaudatus*) crustaceans. *The Biological Bulletin*, **210**(1): 38-50, https://doi.org/10.2307/4134535.

Valanne S, Wang J H, Rämet M. 2011. The *Drosophila* toll signaling pathway. *The Journal of Immunology*, **186**(2): 649-656, https://doi.org/10.4049/jimmunol.1002302.

Voronina M V, Frolova A S, Kolesova E P et al. 2024. The intricate balance between life and death: ROS, cathepsins, and their interplay in cell death and autophagy. *International Journal of Molecular Sciences*, **25**(7): 4087, https://doi.org/10.3390/ijms25074087.

Wang F, Dong S L, Huang G Q et al. 2003. The effect of light color on the growth of Chinese shrimp *Fenneropenaeus chinensis*. *Aquaculture*, **228**(1-4): 351-360, https://doi.org/10.1016/S0044-8486(03)00312-0.

Wang M X, Lu Y, Cai Z Z et al. 2013. Phenol oxidase is a necessary enzyme for the silkworm molting which is regulated by molting hormone. *Molecular Biology Reports*, **40**(5): 3549-3555, https://doi.org/10.1007/s11033-012-2428-8.

Wang X, Wang F, Lu Y L et al. 2014. Effects of light intensity on the respiratory metabolism of swimming crab (*Portunus trituberculatus*). *Journal of Fisheries of China*, **38**(2): 237-243, https://doi.org/10.3724/SP.J.1231.2014.48932. (in Chinese with English abstract)

Weiland A L, Mangum C P. 1975. The influence of environmental salinity on hemocyanin function in the blue crab, *Callinectes sapidus*. *Journal of Experimental Zoology*, **193**(3): 265-273, https://doi.org/10.1002/jez.1401930303.

Wu L L, Wang Y N, Li J et al. 2021. Influence of light spectra on the performance of juvenile turbot (*Scophthalmus maximus*). *Aquaculture*, **533**: 736191, https://doi.org/10.1016/j.aquaculture.2020.736191.

Ye X, Deng Y T, Lai Z C. 2012. Akt is negatively regulated by Hippo signaling for growth inhibition in *Drosophila*. *Developmental Biology*, **369**(1): 115-123, https://doi.org/10.1016/j.ydbio.2012.06.014.

Zhang C S, Li F H, Xiang J H. 2014. Effect of salinity on growth and first sexual maturity of *Exopalaemon carinicauda* (Holthuis, 1950). *Chinese Journal of Oceanology and Limnology*, **32**(1): 65-70, https://doi.org/10.1007/s00343-014-3040-7.

Zhao Q Q, Wei C, Dou J L et al. 2025. Molecular and physiological responses of *Litopenaeus vannamei* to nitrogen and phosphorus stress. *Antioxidants*, **14**(2): 194, https://doi.org/10.3390/antiox14020194.

Zhou H L, Li Y H, Wei L et al. 2014. Sensitivity of larvae and adult and the immunologic characteristics of *Litopenaeus vannamei* under the acute hypoxia. *Journal of Chemistry*, **2014**: 574534, https://doi.org/10.1155/2014/574534.